Elsevier Editorial System(tm) for Remote Sensing of Environment
Manuscript Draft

Manuscript Number:

Title: Hierarchical Mapping of Northern Eurasian Land Cover

Article Type: Full length article

Keywords: Land cover classification; MODIS; biogeography

Corresponding Author: Mr. Damien Sulla-Menashe,

Corresponding Author's Institution: Boston University

First Author: Damien Sulla-Menashe

Order of Authors: Damien Sulla-Menashe; Mark A Friedl; Olga N Krankina; Alessandro Baccini; Curtis E Woodcock; Adam Sibley; Guoqing Sun; Viacheslav Kharuk; Vladimir Elsakov

Hierarchical Mapping of Northern Eurasian Land Cover Using MODIS

Damien Sulla-Menashe[1], Mark A. Friedl[1], Olga N. Krankina[2], Alessandro Baccini[3], Curtis E. Woodcock[1], Adam Sibley[1], Guoqing Sun[4], Viacheslav Kharuk[5] and Vladimir Elsakov[6]

[1]Department of Geography & Environment, Boston University
675 Commonwealth Avenue, Boston, MA 02215, USA.

[2] College of Forestry, Department of Forest Sciences, Oregon State University
202 Richardson Hall, Corvallis, OR 97331-5752, USA.

[3] Woods Hole Research Center
149 Woods Hole Road, Falmouth, MA 02540-1644, USA.

[4] Biospheric Sciences Branch, NASA GSFC

[5] Sukachev Forest Institute, Forest Ecology and Monitoring Branch
Academgorodok Krasnoyarsk, 660036 Russia

[6] Institute of Biology, Komi Science Center, Russian Academy of Sciences,
Kommunisticheskaja st., 28, 167610 Syktyvkar, Russia

Author for correspondence

Damien Sulla-Menashe

Department of Geography and Environment, Boston University

675 Commonwealth Avenue, Boston, MA 02215, USA

Telephone: 617-353-1049

Fax: 617-353-8399

Email: dsm@bu.edu

Submitted for publication in

Remote Sensing of Environment

March 26, 2010

Abstract

The northern Eurasian land mass encompasses a highly diverse array of land cover types including tundra, boreal forest, extensive wetlands, semi-arid steppe, and agricultural land use. Despite the well-established importance of northern Eurasia in the global carbon and climate system, the distribution and properties of land cover in this region are not well characterized. To address this knowledge and data gap, a hierarchical mapping approach was developed for northern Eurasia that encompasses the study area for the Northern Eurasia Earth System Partnership Initiative. The Northern Eurasia Land Cover database developed in this study follows the FAO-Land Cover Classification System and provides nested groupings of land cover characteristics, with separate layers for land use, wetlands, and tundra. Maps were produced using supervised classifications of multi-temporal 500-m surface reflectance and 1-km land surface temperature data from the Moderate Resolution Imaging Spectroradiometer as inputs to an ensemble decision tree algorithm. Climate-vegetation relationships provided complementary information to refine the MODIS-derived classifications. Classification results support the use of hierarchical classification for mapping land cover in this region. Unresolved issues include the need for a more accurate representation of shrub-dominated ecosystems, a better characterization of mixed classes, and the elimination or refinement of false classification dichotomies that cannot be accurately mapped from moderate resolution remote sensing.

1. Introduction

Recent observations suggest that climate change is producing substantial ecological transformations at high latitudes (Serreze et al., 2000; Nemani et al., 2003; Stow et al., 2004; Groisman and Soja, 2009). Northward movement of the treeline and evergreen conifer invasion into larch dominant communities affects the surface radiation balance and the carbon cycle, resulting in both positive and negative feedbacks to the climate system (Kharuk et al., 2007; Bonan, 2008). Similarly, increased rates of soil decomposition and permafrost degradation may substantially modify the carbon balance of the arctic within this century (Davidson and Janssens, 2006; Schuur et al., 2008). Remote sensing has become an essential tool for monitoring ecosystem processes at high latitudes (Myneni et al., 1997; Goetz et al., 2005). By providing indirect measurements of vegetation characteristics, information from remote sensing can help reduce uncertainty in predictions from terrestrial ecosystem models for northern latitude regions (Chapin et al., 1996; Turner et al., 2004; McGuire et al., 2007; Sitch et al., 2007).

Large levels of disagreement exist among current land cover maps of northern Eurasia (Jung et al., 2006; Frey and Smith, 2007). These disagreements can be attributed to differences in mapping methodologies, data sources, mapping errors, and class definitions (Giri et al., 2005). Further, land cover legends are often designed to support user requirements without considering limitations of the data used to perform the classification (Heinl et al., 2009). In this context, two factors complicate the implementation of commonly used land cover classification systems: (1) classes are often included that represent ecological phenomena occurring at different spatial scales, and (2) land cover, land use, and ecoclimatic classes are often incorrectly treated as mutually exclusive entities. These problems reduce the accuracy, utility, and ecological relevance of land cover maps (Latifovic and Olthof, 2004; Jung et al., 2006). Two examples that illustrate these challenges are the representation of high-latitude tundra and wetlands. The tundra biome is difficult to map using remote sensing because of its long winter, patchy composition, and ephemeral snow and water coverage (Stow et al., 2004). Wetlands tend to be under-represented in recent maps because they are treated as a land cover class instead of a hydrologic state characteristic of multiple land cover classes (Frey and Smith, 2007;

Krankina et al., 2008). New strategies are therefore required to resolve these issues, and to produce more consistent land cover characterizations of high latitude regions.

The Northern Eurasia Earth System Partnership Initiative (NEESPI) is an international consortium established to investigate and monitor the effects of human activity and changes to biogeochemical, energy, and water cycles across the northern Eurasia landmass (Groisman and Bartalev, 2007; Groisman et al., 2009). The goal of the Northern Eurasia Land Dynamics Analysis (NELDA) project is to provide a comprehensive characterization of land surface properties in the NEESPI region in support of science questions ranging from climate controls on vegetation productivity to the socio-economic causes and ecological consequences of land-use and land-cover change.

Here we describe the Northern Eurasia Land Cover (NELC) database that was developed for NELDA and addresses several of the issues described above. Specifically, we present a strategy for mapping land cover at continental scale while preserving important ecological details. Our approach follows the FAO-UNEP Land Cover Classification System (LCCS) and provides nested groupings of land cover characteristics (Di Gregario and Jansen, 2000). To map these classes we use moderate spatial resolution (500-m) remote sensing data from NASA's Moderate Resolution Imaging Spectroradiometer (MODIS). The top level of the NELC hierarchy includes information related to broad-scale patterns in biotic and abiotic land surface features. Lower levels distinguish among land cover properties related to vegetation physiognomy. Separate layers complement the land cover hierarchy and include land-use, hydrologic, and ecoclimatic distinctions. The result is a set of mutually exclusive classes that are consistent across spatial scales. Below we describe the legend used by the NELC map, followed by an overview of the classification process and the post-classification refinement steps. In the final sections we assess the accuracy of the NELC database and discuss the strengths and weaknesses of the mapping strategy.

2. NELDA Land Cover Mapping

2.1. Class Definitions

The NELC legend (Tables 1 and 2) was developed to balance the science needs of NEESPI with the capabilities of the MODIS sensor for mapping land cover. The hierarchical structure of the NELC legend is shown in Figure 1. The hierarchy contains three main levels; each providing nested and increasingly refined distinctions relative to the level above it. The distinctions for each level follow the LCCS model according to the criteria described below.

The top level in the hierarchy separates vegetated land (greater than 10 percent vegetation cover) from water bodies, perennial snow and ice, and barren land. The second level divides vegetated land into groups based on the dominant life form and the vegetation cover fraction. Following the LCCS, the NELC legend describes vegetated land as being composed of three life form types: trees, shrubs, and herbaceous vegetation. The dominant life form occupies the upper layer of the canopy with at least 10 percent coverage. Trees are distinguished from shrubs based on a height threshold of five meters. For vegetation under 5 meters, perennial woody shrubs are distinguished from annual herbaceous plants. Following the LCCS, the dominant layer is defined as closed if canopy closure is greater than 60-70 percent; otherwise the canopy is defined as open. Vegetated lands thus encompass six possible combinations of dominant life form and canopy closure (Table 1; Figure 1).

The third level in the hierarchy describes characteristics of life form physiognomy defined by leaf type and leaf phenology. This level contains five possible subclasses of tree-dominated land cover: evergreen broadleaf, deciduous broadleaf, evergreen needleleaf, deciduous needleleaf, and mixed. Of these, evergreen broadleaf trees are not present in the NEESPI region. The mixed class refers to tree-dominated areas with no dominant physiognomy. The shrub-dominated classes can be further sub-divided by their leaf type, and herbaceous land cover can be further sub-divided into graminoid, forb, and lichen/moss; however, in this study we leave out these distinctions, as they could not be accurately mapped from MODIS.

Four classes in the NELC legend do not fit in the nested framework presented above because they are not actual land cover types: urban, cultivated land, wetlands, and tundra. Three additional layers are therefore included in the NELC database that complement the previously described land cover hierarchy and capture distinctions in land-use, hydrologic regime, and eco-climatology (Table 2). The land use layer includes cultivated and urban areas. A location is classified as cultivated if herbaceous cropland covers more than 75 percent of the surface, excluding orchards, vineyards, and pastures. The urban class consists of built up land where buildings or other man-made structures cover more than 15 percent of the area. The wetland class is defined by vegetated land that is permanently or semi-permanently inundated by water. The tundra class is defined as vegetated land above the treeline that is snow-free for 1-3 months of the year. The creation of these extra layers is discussed in Section 2.4.

2.2. Classification Algorithm

The NELC maps were created using supervised classification of MODIS data produced by ensemble decision trees (Breiman et al., 1984; Quinlan, 1996; McIver and Friedl, 2001). The procedure and input data for the NELC classifications are similar to those used for the MODIS land cover product (MCD12Q1; Friedl et al., 2002; 2010). However, we have significantly refined this approach to address issues of class definition and scale specific to the NELC legend. In particular, separate classifications were produced for each level in the NELC hierarchy, providing unique classifications tuned to detect different land cover properties at each level of the classification hierarchy.

High quality exemplars (training sites) for each class are required to estimate the ensemble decision trees. Many of the NELDA training sites were derived from the site database used to produce the MODIS land cover product. Existing sites within the NEESPI region were re-interpreted and labeled to conform to the LCCS-based scheme and the database was augmented to increase representation of under-sampled classes. The final version of the database contained 461 sites, of which approximately 350 were derived from the existing MODIS land cover database. Quality control of existing sites and selection of new sites involved reviewing high-resolution imagery available in GoogleEarth© and

information from the Degree Confluence Project (Iwao et al., 2006). In collaboration with regional experts from Russia, Kazakhstan, and China, 40 sites deemed to have low-confidence labels were reviewed and the training database was revised accordingly.

The input data used to produce the classification were derived from the Moderate Resolution Imaging Spectroradiometer (MODIS) onboard NASA's Aqua and Terra satellites for 2005 and 2006. The MODIS instrument provides data in seven so-called "land bands" useful for monitoring vegetation at moderate (500-m) spatial resolution. Here we used data from the Nadir BRDF-Adjusted Reflectance (NBAR) product (MCD43; Schaaf et al., 2002). The MODIS land surface temperature (LST) product provided additional information at a slightly coarser (1-km) resolution (Wan, 2008). For each month, the highest quality observations were selected from data spanning two years (2005-2006; a total of eight possible 8-day observations for each pixel in each month) based on quality assurance information included with the MODIS NBAR data. These observations were then used to compute the mean and variance in monthly reflectance for each spectral band and LST. Monthly mean reflectances were also used to estimate three indices: the two-band enhanced vegetation index (EVI2; Jiang et al., 2008), the normalized difference wetness index (NDWI; Gao, 1996), and the normalized difference snow index (NDSI; Hall et al., 1995). The brightness, greenness, and wetness components of the MODIS tasseled cap were also provided as input features to the classifications (Lobser and Cohen, 2007). These indices and transformations reflect different biophysical properties of the surface and provide additional discriminatory power for land cover classification.

2.3. Post-Classification Adjustments

Like most classification algorithms, results from ensemble decision tree classifications need to be adjusted for biases and errors. In particular, uneven representation of classes in the training dataset and inadequate class separation in the remote sensing inputs introduce error to the classification results. Correction of the former problem is straightforward: the class-likelihoods produced by the decision trees for each class are adjusted in inverse proportion to that class's frequency in the training dataset (Friedl et al., 2010). Resolving the latter issue is more complex and requires a set of ancillary data layers that provide *a*

priori approximations for the likelihood for each class at each pixel. These prior probability layers can be used to help distinguish spectrally similar classes and provide a "best guess" within areas of significant missing data or where information in MODIS is insufficient (McIver and Friedl, 2002). Production of the prior probability layers used for this work is central to our method and is described in more detail next.

2.4. Prior Probability Layers

The utility of prior probabilities in classification of remotely sensed data has been widely recognized for three decades (Strahler, 1980; Lee et al., 1987; McIver and Friedl, 2002). For this work we used climate-vegetation relationships to estimate prior probabilities for each class at each pixel within the two vegetated levels of the NELC hierarchy. Biomes, which describe broad-scale vegetation patterns, have long been delineated using climate boundaries based on physiological limitations to plant growth and survival (Holdridge, 1947; Mather and Yoshioka, 1968; Box, 1981; Woodward and Williams, 1987; Woodward et al., 2004). Utilizing these relationships we were able to approximately characterize the likelihood of each class' presence at each pixel. While this approach does not consider important ecological factors including competition, soil development, nutrient availability, and disturbance regimes, our approach provides a robust source of ancillary information that effectively complements information derived from remote sensing.

Prior probabilities for vegetation classes corresponding to the NELC classification were created using the same decision tree procedure outlined for the MODIS-based classifications. Specifically, we estimated supervised classifications that yield the likelihood for each class at each pixel. To do this, training data were randomly selected from areas of agreement between two recent land cover maps covering the NEESPI region: the GLC2000 product produced from SPOT4-VEGETATION imagery (Bartalev et al., 2005) and the Collection 5 2004 MCD12Q1 Land Cover Product produced from MODIS imagery (Friedl et al., 2010). These data were used to train ensemble decision trees based on 67 climate variables including monthly extremes and means of air temperature, monthly means of precipitation, and seasonal and annual aggregations of the monthly variables.

Climate data were acquired from the WORLDCLIM dataset (Hijmans et al., 2005). This climatology is based on measurements obtained between 1950-2000 from a global network of meteorological stations and is available at 1-km spatial resolution.

The climate-derived potential vegetation classifications resulted in a set of prior probability layers that were used to adjust the class predictions for the dominant life form and tree-dominated classifications of MODIS data. The adjustment was performed using Bayes' Rule, with the prior probabilities weighted using a user-specified confidence parameter (McIver and Friedl, 2002). The specific value of the weight represents the map producers' confidence in the climate-based predictions to reproduce the actual distribution of mapped classes. Higher confidence was assigned to the prior probabilities for the leaf type and phenology layer than for the dominant life form layer because we expect that natural and anthropogenic-caused disturbances significantly alter both the distribution of the dominant life forms and their cover fractions within the region. Because climate is a relatively poor predictor of non-vegetated land types, prior probabilities for the vegetated and non-vegetated classification were based on class frequencies derived from a 35 x 35 km moving window of the Collection 5 MCD12Q1 product (Friedl et al., 2010). Water bodies were mapped using the 250-m land-water mask produced by Carroll et al. (2009), which integrates spectral information from MODIS with a high-resolution digital elevation model.

To illustrate the nature and effectiveness of the prior probability layers, Figure 2 presents a subset of the climate-derived prior probability layers for the northern Eurasia landmass. The color scheme of these images represents the class-specific prior probability value at every pixel. In the two top images, areas labeled as N/A refer to non-vegetated land. In the bottom two images, N/A refers to non-vegetated land as well as land dominated by non-tree life-forms. The tree-closed prior probability layer shows that the climate in many Eastern European countries and in western Russia is well-suited for forest, much of which has been cleared over many generations for agriculture. The tree-open layer captures the taiga-tundra transition zone in the north, with a sharp transition along the forest-steppe boundary to the south. Both the evergreen needleleaf and deciduous

broadleaf prior probability layers realistically depict the geographic distributions of these classes, but tend to over-estimate both classes in larch-dominated regions of Siberia.

2.5. Production of Additional NELC Layers

In addition to land cover, the NELC legend includes three additional complementary layers: land use (which includes agricultural and urban areas), wetlands, and tundra. To map agricultural land use, a separate classification of cultivated versus non-cultivated land was performed using MODIS data, but restricted to herbaceous land cover. A global map of agricultural intensity (Ramankutty et al., 2008) derived from a combination of remotely sensed and national survey data served as a prior probability layer for this classification. The urban land use layer was derived from the global map of urban land areas produced by Schneider et al. (2009). The wetland layer includes results from two separate MODIS-based classifications: one for herbaceous wetlands, the other grouping tree and shrub-dominated land cover into a single woody life form type. Classification results for the wetland and agriculture classes were adjusted to reduce over-prediction of these relatively uncommon classes. To be conservative, pixels belonging to these classes were relabeled if they were predicted with posterior probabilities lower than 90% and 80%, respectively.

The tundra layer was created using five-year (2001-2005) monthly means of the MODIS normalized difference snow index (NDSI), a two-band spectral transformation that is particularly sensitive to snow (Hall et al., 1995; Salomonson and Appel, 2004). Tree-dominated or non-vegetated pixels were excluded from the analysis. The average annual snow-free period was calculated by counting the number of summer months above a threshold of 0.32 in monthly mean NDSI. This threshold is lower than the NDSI threshold of 0.4 used by the MODIS snow cover product but is within the range expected for snow-covered pixels (Hall et al., 1995). Mean values for the twenty 8-day observations during each month over the five-year period at each pixel provide a conservative estimate of snow cover and visual inspection suggested that this lower threshold was appropriate for the northern Eurasia study region.

3. Accuracy Assessment of the NELC Database

In this section we present an accuracy assessment of the NELC database, including the land use and wetland layers. To do this, a 10-fold cross-validation analysis was performed using a procedure similar to the one used to assess the MODIS C5 Land Cover product (Friedl et al., 2010). Results from the cross-validation analysis are summarized in Table 3 and are presented as a series of error matrices compiled at each level of the hierarchy (Tables 4-8). In future work, the NELC product will be validated using independent test sites across Northern Eurasia that have been classified using Landsat TM imagery upscaled to the spatial resolution of MODIS (Krankina et al., 2008).

The NELC classification scheme includes 15 classes for the NEESPI region (Table 1; Figure 3). To perform the cross-validation, the NELC training data was randomly split into ten subsets, keeping pixels from individual sites together (Friedl et al., 2000). Using these subsets we cross-validated classification results at each level in the classification hierarchy. Comparisons between the predicted and the training site labels were used to compute class-specific accuracies and standard errors adjusted for cluster sampling following Stehman (1997). In interpreting the results presented in Tables 3-9 it is important to note that the accuracy statistics contain errors resulting from subjective labeling of the training dataset, classifier biases caused by small sample sizes and non-random sampling, and challenges presented by mixed pixels (Foody, 2002). Further, while the cross-validation procedure provides a randomization of training and test data, the sample distribution is not based on a probability-design, and results need to be interpreted in this context. Despite these issues, the overall accuracies summarized in Table 3 and the error matrices presented in Tables 4-8 are useful in assessing overall map quality, characterizing confusion between classes, and identifying potential problems arising from the training data.

The overall accuracy for the top level of the hierarchy is 98.5 percent correctly classified, and for the dominant life form and cover fraction layer, the accuracy is 78.5 percent (Table 3). The error matrix for this second layer indicates two issues with the classification results: confusion between the “open” and “closed” cover fraction classes for

each life-form and difficulty in mapping shrubland ecosystems (Table 5). Errors of commission for the tree-open and herbaceous classes are related to confusion with their closed tree and herbaceous counterparts, and suggest limited spectral separability between these class pairs in MODIS data. Mislabeling of tree-open training sites as tree-closed land cover may contribute to over-estimation of the tree-closed class. In a related study, Montesano et al. (2009) suggest that MODIS-based predictions of tree cover fraction overestimate actual tree cover in the taiga-tundra transition zone, which is consistent with our results.

Overall accuracies for the leaf type and phenology layers are 75.3 percent for the tree-open classification and 79.2 percent for the tree-closed classification (Table 3). Large standard errors in the class-specific accuracies of the tree-open classification (Table 6) arise partly from small training sample sizes, but also suggest that it may not be possible to confidently distinguish leaf type and phenology for high latitude woodlands using moderate spatial resolution data such as MODIS. The spectral signature of an open canopy of trees is strongly influenced by understory characteristics that substantially complicate the classification problem. More uniform classes, such as those within the tree-closed sub-group, have more separable spectral-temporal signatures.

The overall accuracy for the agriculture layer is 72.6 percent, and the herbaceous and woody wetland classifications have accuracies of 90.1 and 93.8 percent, respectively (Table 3). Classification accuracies for the agriculture and wetland classes are affected by post-classification adjustments specific to these classes, as described in Section 2.4. These adjustments increased errors of omission for the agriculture and herbaceous wetland classes relative to the unadjusted decision tree results: some agriculture and wetland pixels were incorrectly mapped as natural vegetation and dryland, respectively, but fewer natural and dryland pixels were incorrectly mapped as agriculture and wetland (Tables 7 and 8).

4. Assessment of the Land Cover Hierarchy and the Prior Probability Layers

Hierarchical classification provides a method for mapping complex vegetation types using a series of simpler decisions, improving both the final map quality and the ecological

meaning of each class (Dai and Khorram, 1998). In this section we present results from two analyses that evaluate the effectiveness of the hierarchical and Bayesian classification model used for this work. To do this, we first compare classification accuracies from the hierarchical classification to those from an ensemble decision tree classification that produces all 15 land cover classes in one step. Second, we assess how and where the use of prior probabilities affect classification results. As part of this latter analysis, we examine the efficacy of using climate data as a basis for estimating prior probabilities for vegetated classes in the NELC database.

To do the first analysis, the cross-validation procedure described in Section 3 was performed on classification results from a non-hierarchical classifier that produced all 15 classes at the same time. The results from this cross-validation were then compared with results of the hierarchical classification for each class (Table 9). Note that the results presented for the hierarchical classification are not identical to those presented in Section 3 (Tables 4-8), which had been adjusted for the two sources of bias described in Section 2.3. To make the comparison more direct, we did not apply these adjustments here.

The results presented in Table 9 reveal substantial differences between the classifications produced by each approach. Most importantly errors of omission are substantially reduced for many of the tree-open and tree-closed sub-classes in the hierarchical classification. Similarly, errors of commission are lower for the tree-open sub-classes. The hierarchical model yields relatively few improvements for classes at higher levels of the hierarchy and there is actually a small decrease in accuracy for the shrub-open class. In general, the results suggest that hierarchical stratification of classes presents a set of simpler decisions to the classifier, and is particularly helpful for discriminating between rare classes with narrow thematic definitions: e.g., within the tree-open sub-group.

The posterior probabilities produced by the classification algorithm can be used to visualize patterns of uncertainty in the classification and complement the results from cross-validation (McIver and Friedl, 2001). To summarize information captured by these confidence values we randomly sampled 7,680 pixels (<0.01%) from the NEESPI region. For each level of the hierarchy we extracted the class label, the prior probability value, and

the class likelihoods before and after applying Bayes' rule. The results reveal patterns that illustrate the benefits and limitations of both our method and MODIS data for mapping classes included in the NELC legend. In addition to the analysis of posterior probabilities, we explored the influence of climate-derived prior probability layers on the final confidence values.

Boxplots showing the final posterior probabilities for the land cover hierarchy are presented in Figure 4. Because each layer in the hierarchy provides a successively refined characterization of land cover types, posterior probabilities decrease at lower levels in the hierarchy. The mean posterior probability at the top level of the hierarchy is 94.8 percent. The mean at the second level (dominant life form and cover fraction) is 67.9 percent. This result reflects the more limited spectral separability of these classes in MODIS data relative to the top level. For the leaf type and phenology layer, the mean probabilities of the tree-open and tree-closed classifications are 68.1 and 62.2 percent, respectively.

At the top level of the hierarchy the vegetation and water classes are clearly classified with higher confidence relative to the snow/ice and barren classes. The latter classes dominate the high Arctic and alpine regions, and identification of these classes is difficult because of high proportions of missing data caused low solar zenith angles during the winter and imperfect cloud screening, especially for the snow/ice class (see errors of commission in Table 9). Not surprisingly the distribution of posterior probabilities for the life form and cover fraction layer shows a similar pattern to the class accuracies for this layer (Figure 4; Table 5). Lower classification accuracies for the shrub and tree-open classes are reflected in corresponding low probability values, and are associated with spectral confusion between shrubs and trees and between shrubs and herbaceous vegetation (Table 5).

To examine this issue further we use a metric designed to measure the effect of the climate-derived prior probability layers. This metric, which we call the Normalized Margin Difference (NMD), uses the margin (i.e., the difference in conditional or posterior probabilities) for the two most likely classes as a measure of class separability. The Normalized Margin Difference (NMD) is calculated by taking the difference between the

margins before and after applying the prior probabilities and normalizing this difference by their sum: $NMD = \frac{M_B - M_A}{M_B + M_A}$, where M_B and M_A represent the margins before and after.

Since the climate-derived prior probability layers are responsible for changes in posterior probabilities relative to the ensemble decision tree results, the NMD provides a measure of the contribution of the prior probability layers to class separability. Boxplots showing the distribution of the NMD across the second and third layers of the hierarchy are shown in Figure 5. Values around zero indicate that the prior probabilities had relatively little effect; positive values indicate that the prior probabilities improved class separability and vice versa. In this context, it is important to note that because the influence of the prior probabilities is down-weighted (Section 2.4), the magnitude of M_B-M_A is necessarily small.

The influence of the prior probabilities for the life form and cover fraction layer was relatively minor and depended on the specific class. NMD values were modestly positive for the tree-open class and slightly negative for the shrub-closed class (Figure 5). The narrow response of the NMD for these classes can be largely attributed to the low weight assigned to its prior probability layer. In contrast, the use of prior probabilities produced significant improvements in class separability in the tree-closed classification for both the deciduous broadleaf and evergreen needleleaf classes. Among the tree-open classes the NMD values are strongly positive for the evergreen needleleaf class and slightly negative for the mixed class. Overall, the climate-vegetation relationships captured via prior probabilities reduce classification uncertainty. This is especially important for those classes that have limited spectral separability in MODIS data but that can be effectively delineated by climate variables: e.g., between the deciduous needleleaf and deciduous broadleaf tree classes.

5. Discussion and Conclusions

We present a hierarchical strategy for mapping northern Eurasian land cover that includes separate map layers for land use (urban, agriculture), wetlands, and tundra. The resulting Northern Eurasia Land Cover (NELC) database provides a source of information for regional land cover in support of NEESPI-related projects. The FAO-LCCS was used as a

basis for developing the land cover legend and in formalizing distinctions among the land cover, land use, tundra and wetlands classes included in the database. Ensemble decision trees were used to produce classifications for each level of the hierarchy. These results were then corrected for biases inherent to the classification approach using methods similar to those used to produce the MODIS global land cover type product.

The mapping strategy used for this work implemented two novel strategies that proved to be effective. First, a classification strategy was used that is consistent with the hierarchical structure of the FAO-LCCS. Second, climate-vegetation relationships were used as a source of ancillary information to help distinguish classes with limited spectral separability in MODIS data. Inspection of classification results indicates that the hierarchical approach presents a set of simpler decisions to the classifier, thereby improving map quality. In particular, fusing information from MODIS with climate data at lower levels of the hierarchy improved our ability to describe ecologically important phenomena at the relatively coarse scale of MODIS pixels. We therefore conclude that improvements to the hierarchical design and the implementation of ancillary information have the potential to further reduce classification uncertainty. Unresolved issues include how to represent mixture classes, how to better incorporate ancillary information, and how to improve the map based on feedback from the public.

The most difficult challenge encountered during the creation of the NELC database was in mapping shrub-dominated ecosystems. These ecosystems exist in three broad climate zones of northern Eurasia: arid areas of the central steppes, the tundra-taiga transition, and in the tundra zone itself (Figure 3). In the first case there is significant spectral confusion between perennial xeric shrubs and open herbaceous vegetation. In the second case, closed shrublands are confused with open larch woodlands in central Siberia. In these environments harsh seasonal climates limit tree stature and dense understories of shrubs and grasses may further confuse the spectral signature. The third case is perhaps the most challenging to resolve: the tundra biome contains ecosystems with patchy mixtures of perennial shrubs, annual forbs, grasses, sedges, mosses, and lichens. The limited spectral separability of these life forms is compounded by the short Arctic growing season. To help resolve these challenges, we suggest two strategies that could help to

characterize tundra vegetation and shrub-dominated ecosystems in general. First, the life form and cover fraction level of the hierarchy could be refined to better exploit the information content of MODIS data. For example, shrubs could be considered sub-classes of woody and herbaceous-dominated classes and classified in a separate step. Second, more work is needed to devise more effective means of including climate information such as the summer isotherm to identify tundra zones of similar vegetation forms (Walker, 2000).

Acknowledgements

The research was supported by NASA grant numbers NNG06GF54G and NNX08AE61A. An additional thanks goes to Dr. Bin Tan who was instrumental in implementing the MODIS classification algorithms, and to the rest of the NELDA team for helpful input and discussions.

References

Bartalev, S. A., Belward, A. S., Erchov, D. V., & Isaev, A. S. (2003). A new SPOT4-VEGETATION derived land cover map of Northern Eurasia. *International Journal of Remote Sensing, 24* (9), 1977-1982.

Bonan, G. B. (2008). Forests and climate change: forcings, feedbacks, and the climate benefits of forests. *Science, 320,* 1444-1449.

Box, E. O. (1981). Predicting physiognomic vegetation types with climate variables. *Plant Ecology, 45* (2), 127-139.

Breiman, L, Friedman, J. H., Olshen, R. A., & Stone, C. J. (1984). *Classification and Regression Trees.* Relmont, CA: Wadsworth.

Carroll, M. L., Townshend, J. R., DiMiceli, C. M., Noojipady, P., & Sohlberg, R. A. (2009). A new global raster water mask at 250 meter resolution. *International Journal of Digital Earth, 2,* (4), 291-308.

Chapin, F. S., Bret-Harte, M. S., Hobbie, S. E., & Zhong, H. (1996). Plant functional types as predictors of transient responses of arctic vegetation to global change. *Journal of Vegetation Science, 7* (3), 347-358.

Dai, X., & Khorram, S. (1998). A hierarchical methodology framework for multisource data fusion in vegetation classification. *International Journal of Remote Sensing, 19* (18), 3697-3701.

Davidson, E. A., & Janssens, I. A. (2006). Temperature sensitivity of soil carbon decomposition and feedbacks to climate change. *Nature, 440,* 165-173.

Di Gregario, A., & Jansen, L. J. M. (2000). *Land Cover Classification System (LCCS): Classification Concepts and User Manual*. Rome: Food and Agriculture Organization of the United Nations.

Foody, G. M. (2002). Status of land cover classification accuracy assessment. *Remote Sensing of the Environment, 80* (1), 185-201.

Frey, K. E., & Smith, L. C. (2007). How well do we know northern land cover?: Comparison of four global vegetation and wetland products with a new ground-truth database for West Siberia. *Global Biogeochemical Cycles, 21,* GB1016, doi: 10.1029/2006GB002706.

Friedl, M. A., Woodcock, C., Gopal, S., Muchoney, D., Strahler, A. H., & Barker-Schaaf, C. (2000). A note on procedures used for accuracy assessment in land cover maps derived from AVHRR data. *International Journal of Remote Sensing, 21* (5), 1073-1077.

Friedl, M. A., McIver, D. K., Hodges, J. C. F., Zhang, X. Y., Muchoney, D., Strahler, A. H., Woodcock, C. E., Gopal, S., Schneider, A., & Cooper, A. (2002). Global land cover mapping from MODIS: Algorithms and early results. *Remote Sensing of Environment, 83* (1), 287-302.

Friedl, M. A., Sulla-Menashe, D., Tan, B., Schneider, A., Ramankutty, N., Sibley, A., & Huang, X. (2010). MODIS collection 5 global land cover: Algorithm refinements and characterization of new datasets. *Remote Sensing of Environment, 114* (1), 168-182.

Gao, B. C. (1996). NDWI – A normalized difference water index for remote sensing of vegetation liquid water from space. *Remote Sensing of Environment, 58* (3), 257-266.

Giri, C., Zhou, Z., & Reed, B. (2005). A comparative analysis of the Global Land Cover 2000 and MODIS land cover data sets. *Remote Sensing of Environment, 94* (1), 123-132.

Goetz, S. J., Bunn, A. G., Fiske, G. J., & Houghton, R. A. (2005). Satellite-observed photosynthetic trends across boreal North America associated with climate and fire disturbance. *Proceedings of the National Academy of Sciences, 102* (38), 13521-13525.

Groisman, P. Y., & Bartalev, S. A. (2007). Northern Eurasia Earth Science Partnership Initiative (NEESPI) science plan overview. *Global and Planetary Change, 56,* (3-4), 215-234.

Groisman, P., & Soja, A. J. (2009). Ongoing climatic change in northern Eurasia: Justification for expedient research. *Environmental Research Letters, 4,* 045002, doi: 10.1088/1748-9326/4/4/045002.

Groisman, P. Y., Clark, E. A., Kattsov, V. M., Lettenmaier, D. P., Sokolik, I. N., Aizen, V. B., Cartus, O., Chen, J., Conard, S., Katzenberger, J., Krankina, O., Kukkonen, J., Machida, T., Maksyutov, S., Ojima, D., Qi, J., Romanovsky, V. E., Santoro, M., Schmullius, C. C., Shiklomanov, A. I., Shimoyama, K., Shugart, H. H., Shuman, J. K., Sofiev, M. A., Sukhinin, A. I., Vorosmarty, C., Walker, D., & Wood, E. F. (2009). The Northern Eurasia Earth Science

Partnership: An example of science applied to societal needs. *Bulletin of the American Meteorological Society 90,* (5), 671-688.

Hall, D. K., Riggs, G. A., & Salomonson, V. V. (1995). Development of methods for mapping global snow cover using Moderate Resolution Imaging Spectroradiometer data. *Remote Sensing of Environment, 54* (2), 127-140.

Heinl, M., Walde, J., Tappeiner, G., & Tappeiner, U. (2009). Classifiers vs. input variables – The drivers in image classification for land cover mapping. *International Journal of Applied Earth Observation and Geoinformation, 11,* 423-430.

Hijmans, R. J., Cameron, S. E., Parra, J. L., Jones, P. G., & Jarvis, A. (2005). Very high resolution interpolated climate surfaces for global land areas. *International Journal of Climatology, 25* (15), 1965-1978.

Holdridge, L. R. (1947). Determination of world plant formations from simple climatic data. *Science, 105,* 367-368.

Iwao, K., Nishida, K., Kinoshita, T., & Yamagata, Y. (2006). Validating land cover maps with Degree Confluence Project information. *Geophysical Research Letters, 33,* L23404, doi: 10.1029/2006GL027768.

Jiang, Z., Huete, A. R., Didan, K, & Miura, T. (2008). Development of a two-band enhanced vegetation index without a blue band. *Remote Sensing of Environment 112,* (10), 3333-3843.

Jung, M., Henkel, K., Herold, M., & Churkina, G. (2006). Exploiting synergies of global land cover products for carbon cycle modeling. *Remote Sensing of Environment, 101* (4), 534-553.

Kharuk, V., Ranson, K., & Dvinskaya, M. (2007). Evidence of evergreen conifer invasion into larch dominated forests during recent decades in central Siberia. *Eurasian Journal of Forest Research, 10* (2), 163-171.

Krankina, O. N., Pflugmacher, D., Friedl, M., Cohen, W. B., Nelson, P., & Baccini, A. (2008). Meeting the challenge of mapping peatlands with remotely sensed data. *Biosciences Discussions, 5,* 2075-2101.

Latifovic, R., & Olthof, I. (2004). Accuracy assessment using sub-pixel fractional error matrices of global land cover products derived from satellite data. *Remote Sensing of Environment, 90* (2), 153-165.

Lee, T., Richards, J. A., & Swain, P. H. (1987). Probabilistic and evidential approaches for multisource data analysis. *IEEE Transactions on Geoscience and Remote Sensing, 25,* (3), 283-292.

Lobser, S. E., & Cohen W. B. (2007). MODIS tasseled cap: Land cover characteristics expressed through transformed MODIS data. *International Journal of Remote Sensing, 28* (22), 5079-5101.

Mather, J. R., & Yoshioka, G. A. (1968). The role of climate in the distribution of vegetation. *Annals of the Association of American Geographers, 58,* 29-41.

McGuire, A. D., Chapin, F. S., Wirth, C., Apps, M., Bhatti, J., Callaghan, T., Christensen, T. R., Clein, J. S., Fukuda, M., Maximov, T., Onuchin, A., Shvidenko, A., & Vaganov, E. (2007). Responses of high latitude ecosystems to global change: Potential consequences for the climate system. In J. G. Canadell, D. E. Pataki, & L. F. Pitelka (Eds.), *Terrestrial Ecosystems in a Changing World* (pp. 297-310). Berlin, Germany: Springer-Verlag.

McIver, D. K., & Friedl, M. A. (2001). Estimating pixel-scale land cover classification confidence using nonparametric machine learning methods. *IEEE Transactions on Geoscience and Remote Sensing, 39* (9), 1959-1968.

McIver, D. K., & Friedl, M. A. (2002). Using prior probabilities in decision-tree classification of remotely sensed data. *Remote Sensing of Environment, 81* (2-3), 253-261.

Montesano, P. M., Nelson, R., Sun, G., Margolis, H., Kerber, A., & Ranson, K. J. (2009). MODIS tree cover validation for the circumpolar taiga-tundra transition zone. *Remote Sensing of Environment, 113* (10), 2130-2141.

Myneni, R. B., Keeling, C. D., Tucker, C. J., Asrar, G., & Nemani, R. R. (1997). Increased plant growth in the northern high latitudes from 1981 to 1991. *Nature, 386,* 698-702.

Nemani, R. R., Keeling, C. D., Hashimoto, H., Jolly, W. M., Piper, S. C., Tucker, C. J., Myneni, R. B., & Running, S. W. (2003). Climate-driven increases in global terrestrial net primary production from 1982 to 1999. *Science, 300,* 1560-1563.

Quinlan, J. R. (1996). Bagging, boosting, and C4.5. *Proceedings of the 1996 Thirteenth National Conference on Artificial Intelligence,* Portland, OR, 04-06 August 1996, pp. 725-730.

Ramankutty, N., Evan, A. T., Monfreda, C., & Foley, J. A. (2008). Farming the planet: 1. The geographic distribution of global agricultural lands in the year 2000. *Global Biogeochemical Cycles, 22* (1), GB1003, doi: 10.1020/2007GB002952.

Salomonson, V. V., & Appel, I. (2004). Estimating fractional snow cover from MODIS using the normalized difference snow index. *Remote Sensing of Environment, 89* (3), 351-360.

Schaaf, C. B., Gao, F., Strahler, A. H., Lucht, W., Li, X., Tsang, T., Strugnell, N. C., Zhang, X., Jin, Y., Muller, J. P., Lewis, P., Barnsley, M., Hobson, P., Disney, M., Roberts, G., Dunderdale, M., Doll, C., d'Entremont, R., Hu, B., Liang, S., & Privette, J. L. (2002). First operational BRDF, albedo and nadir reflectance products from MODIS. *Remote Sensing of Environment, 83* (1-2), 135-148.

Schneider, A., Friedl, M. A., & Potere, D. (2009). A new map of global urban extent from MODIS data. *Environmental Research Letters, 4,* 044003, doi: 10.1088/1748-9326/4/4/044003.

Schuur, E. A. G., Bockheim, J., Canadell, J. G., Euskirchen, E., Field, C. B., Goryachkin, S. V., Hagemann, S., Kuhry, P., Lafleur, P. M., & Lee, H. (2008). Vulnerability of permafrost carbon to climate change: Implications for the global carbon cycle. *Bioscience, 58* (8), 701-714.

Serreze, M. C., Walsh, J. E., Chapin, F. S., Osterkamp, T., Dyurgerov, M., Romanovsky, V., Oechel, W. C., Morison, J., Zhang, T., & Barry, R. G. (2000). Observational evidence of recent change in the northern high-latitude environment. *Climatic Change, 46* (1), 159-207.

Sitch, S., McGuire, A. D., Kimball, J., Gedney, N., Gamon, J., Engstrom, R., Wolf, A., Zhuang, Q., Clein, J., & McDonald, K. C. (2007). Assessing the carbon balance of circumpolar Arctic tundra using remote sensing and process modeling. *Ecological Applications, 17* (1), 213-234.

Stehman, S. V. (1997). Estimating standard errors of accuracy assessment statistics under cluster sampling. *Remote Sensing of Environment, 60* (3), 258-269.

Stow, D. A., Hope, A., McGuire, D., Verbyla, D., Gamon, J., Huemmrich, F., Houston, S., Racine, C., Sturm, M., Tape, K., Hinzman, L., Yoshikawa, K., Tweedie, C., Noyle, B., Silapaswan, C., Douglas, D., Griffith, B., Jia, G., Epstein, H., Walker, D., Daeschner, S., Peterson, A., Zhou, L., & Myneni, R. (2004). Remote sensing of vegetation and land-cover change in Arctic Tundra Ecosystems. *Remote Sensing of Environment, 89* (3), 281-308.

Strahler, A. H. (1980). The use of prior probabilities in maximum likelihood classification of remotely sensed data. *Remote Sensing of Environment, 10* (2), 135-163.

Turner, D. P., Ollinger, S. V., & Kimball, J. S. (2004). Integrating remote sensing and ecosystem process models for landscape- to regional-scale analysis of the carbon cycle. *Bioscience, 54* (6), 573-584.

Walker, D. A. (2000). Hierarchical subdivision of Arctic tundra based on vegetation response to climate, parent material, and topography. *Global Change Biology, 6* (Suppl. 1), 19-34.

Wan, Z. (2008). New refinements and validation of the MODIS land-surface temperature/emissivity products. *Remote Sensing of Environment, 112* (1), 59-74.

Woodward, F. I., & Williams, B. G. (1987). Climate and plant distribution at global and local scales. *Plant Ecology, 69* (1), 189-197.

Woodward, F. I., Lomas, M. R., & Kelly, C. K. (2004). Global climate and the distribution of plant biomes. *Philosophical Transactions of the Royal Society B, 359* (1450), 1465-1476.

Figure 1. Hierarchical structure of the NELC land cover legend. Dashed lines separate different levels in the hierarchy. The land-use, wetland, and tundra layers (not shown) are complementary to the land cover hierarchy.

Figure 2. Prior probability layers derived from climate-vegetation relationships for selected classes. The range of values for each color refers to 100 x the probability (%) of a class' presence at a specific pixel location.

Figure 3. The NELC land cover map including the 15 vegetated and non-vegetated classes. Land use, wetlands, and tundra classes are not shown.

Figure 4. Boxplots showing the distribution of posterior probabilities for each land cover class across a random sample of pixels. For the vegetated and non-vegetated layer: veg refers to vegetated land. For the dominant life form and cover fraction layer: t-o refers to tree-open, t-c to tree-closed, s-o to shrub-open, s-c to shrub-closed, h-o to herbaceous-open, and h-c to herbaceous-closed. For the leaf type and phenology layers: d-bl refers to deciduous broadleaf, e-nl to evergreen needleleaf, and d-nl to deciduous needleleaf.

Figure 5. Boxplots showing the distribution of the Normalized Margin Difference (NMD) metric across a random sample of pixels. The NMD quantifies the relative influence of the climate-derived prior probability layers on the final posterior probabilities. For the dominant life form and cover fraction layer: t-o refers to tree-open, t-c to tree-closed, s-o to shrub-open, s-c to shrub-closed, h-o to herbaceous-open, and h-c to herbaceous-closed. For the leaf type and phenology layers: d-bl refers to deciduous broadleaf, e-nl to evergreen needleleaf, and d-nl to deciduous needleleaf.

Table 1. The legend for the land cover map. The code column represents the coded value of each class in the land cover layer of the NELC database.

Table 2. The legend for the land use, wetlands, and tundra layers. The code column represents the coded value of each class in its respective layer in the NELC database.

Table 3. Summary of user and producer accuracies with standard errors for each layer of the database based on cross-validation.

Table 4. Confusion matrix for the vegetated and non-vegetated layer based on cross-validation. User and producer accuracies with their standard errors are also shown for each class.

Table 5. Confusion matrix for the dominant life form and cover fraction layer based on cross-validation. User and producer accuracies with their standard errors are also shown for each class.

Table 6. Confusion matrix for the leaf type and phenology layer for both the tree-open and tree-closed classifications based on cross-validation. User and producer accuracies

with their standard errors are also shown for each class. Note that confusion is only possible within the tree-open or tree-closed sub-groupings.

Table 7. Confusion matrix for the agriculture layer based on cross-validation. User and producer accuracies with their standard errors are also shown for each class.

Table 8. Confusion matrix for the wetland layer for both the woody wetland and herbaceous wetland classifications based on cross-validation. User and producer accuracies with their standard errors are also shown for each class. Note that confusion is only possible within the woody or herbaceous wetland sub-groupings.

Table 9. Comparison between the user and producer accuracies and standard errors for specific classes according to the hierarchical approach (HIER) and an all-in-one classification (ALL). The tree open - deciduous broadleaf class was omitted by the ALL classification. Note the results for the hierarchical approach are not identical to the confusion matrices presented in Tables 4-8, which had been adjusted for the two sources of bias described in Section 2.3.

Table 1. The legend for the land cover map. The code column represents the coded value of each class in the land cover layer of the NELC database.

Class Name	Code	Class Definition
Tree Dominated		
Tree Closed – Evergreen Needleleaf	1	The crown cover is more than (60-70)%. The height is greater than 5m.
Tree Open – Evergreen Needleleaf	2	The crown cover is between (10-20) and (60-70)%. The height is greater than 5m.
Tree Closed – Deciduous Needleleaf	3	The crown cover is more than (60-70)%. The height is greater than 5m.
Tree Open –Deciduous Needleleaf	4	The crown cover is between (10-20) and (60-70)%. The height is greater than 5m.
Tree Closed – Deciduous Broadleaf	5	The crown cover is more than (60-70)%. The height is greater than 5m.
Tree Open – Deciduous Broadleaf	6	The crown cover is between (10-20) and (60-70)%. The height is greater than 5m.
Tree Closed – Mixed	7	Areas dominated by trees where neither deciduous broadleaved or needleleaved nor evergreen needleleaved species represent > 75% of the tree cover present. The crown cover is more than (60-70)%. The height is greater than 5m.
Tree Open – Mixed	8	Areas dominated by trees where neither deciduous broadleaved or needleleaved nor evergreen needleleaved species represent > 75% of the tree cover present. The crown cover is between (10-20) and (60-70)%. The height is greater than 5m.
Shrub Dominated		
Shrub Closed	9	The crown cover is more than (60-70)%. The height is in the range of 0.3 - 5m.
Shrub Open	10	The crown cover is between (10-20) and (60-70)%. The height is in the range of 0.3 - 5m.
Herbaceous Dominated		
Herbaceous Closed	11	The crown cover is more than (60-70)%. The height is less than 3m.
Herbaceous Open	12	The crown cover is between (10-20) and (60-70)%. The height is less than 3m.
Non-Vegetated		
Barren	13	Non-vegetated areas of exposed soil, sand, or rock containing less than 15% vegetation cover during at least 10 months a year.
Permanent Snow and Ice	14	The land cover consists of perennial snow and ice for a period > 11 months.
Water	15	The land cover consists of perennial natural water bodies where water is present > 11 months.

Table 2. The legend for the land use, wetlands, and tundra layers. The code column represents the coded value of each class in its respective layer in the NELC database.

Layer	Class Name	Code	Definition
1. Human Land Use	Natural herbaceous or pasture	1	Herbaceous areas not cultivated for food production.
	Cultivated land	2	Peak cultivated herbaceous vegetation accounts for 75-100% of the cover.
	Urban	3	Land cover consists of built up areas where buildings or man-made structures cover > 15% of the area.
2. Wetlands	Non-wetland vegetation	1	Vegetation that is inundated with water <4 months annually.
	Herbaceous dominated wetland	2	Herbaceous dominated vegetation inundated with water >4 months annually.
	Woody plant dominated wetland	3	Tree or shrub dominated vegetation inundated with water > 4 months annually.
3. Tundra	Non-tundra herbaceous or shrub	1	Herbaceous or shrub dominated vegetation that is snow free > 3 months of the year.
	Lowland tundra	2	Herbaceous or shrub dominated vegetation that is snow free between 1-3 months of the year. Elevation is < 500m.
	Alpine tundra	3	Herbaceous or shrub dominated vegetation that is snow free between 1-3 months of the year. Elevation is > 500m.

Table 3. Summary of user and producer accuracies with standard errors for each layer of the database based on cross-validation.

		User's Accuracy (Errors of Omission)	Producer's Accuracy (Errors of Commission)
Vegetated and Non-Vegetated		98.5±0.1	98.5±0.1
Life Form and Cover Fraction		78.5±6.4	76.5±4.8
Leaf Type and Phenology	Tree - Open	75.3±13.1	64.3±30.9
	Tree - Closed	79.2±7.2	78.9±7.3
Agriculture		72.6±16.1	91.4±3.3
Wetlands	Herbaceous Wetlands	90.1±6.9	96.5±2.8
	Woody Wetlands	93.8±2.8	89.2±3.3

Table 4. Confusion matrix for the vegetated and non-vegetated layer based on cross-validation. User and producer accuracies with their standard errors are also shown for each class.

TRUE / PRED	Barren	Snow/Ice	Water	Vegetated	User's Accuracy
Barren	237	8	0	17	90.5±10.4
Snow/Ice	0	37	0	0	100
Water	0	0	668	0	100
Vegetated	28	5	1	5729	99.4±0.6
Producer's Accuracy	89.4±11.7	74±48.4	99.9±0.3	99.7±0.4	

Table 5. Confusion matrix for the dominant life form and cover fraction layer based on cross-validation. User and producer accuracies with their standard errors are also shown for each class.

PRED \ TRUE		Tree		Shrub		Herbaceous		User's Accuracy
		Open	Closed	Open	Closed	Open	Closed	
Tree	Open	210	63	32	88	5	67	45.2±17.2
	Closed	241	2174	43	29	0	19	86.8±6.8
Shrub	Open	0	13	78	37	2	119	31.3±28.8
	Closed	8	0	3	86	0	24	71.1±24.4
Herbaceous	Open	1	0	26	0	173	42	71.5±22.2
	Closed	50	23	33	28	238	1797	82.8±12.4
Producer's Accuracy		41.1±13.9	95.6±3.1	36.3±20.5	32.1±18.3	41.4±34.6	86.9±7.4	

Table 6. Confusion matrix for the leaf type and phenology layer for both the tree-open and tree-closed classifications based on cross-validation. User and producer accuracies with their standard errors are also shown for each class. Note that confusion is only possible within the tree-open or tree-closed sub-groupings.

PRED \ TRUE		Evergreen Needleleaf		Deciduous Needleleaf		Deciduous Broadleaf		Mixed		User's Accuracy
		Open	Closed	Open	Closed	Open	Closed	Open	Closed	
Evergreen Needleleaf	Open	55	--	0	--	0	--	20	--	66.7±38
	Closed	--	596	--	6	--	0	--	73	88.3±10.6
Deciduous Needleleaf	Open	0	--	80	--	9	--	1	--	88.9±14.8
	Closed	--	14	--	404	--	0	--	9	94.6±7.3
Deciduous Broadleaf	Open	0	--	28	--	25	--	9	--	46.3±62
	Closed	--	0	--	8	--	582	--	84	86.4±11
Mixed	Open	52	--	7	--	11	--	35	--	33.7±29.5
	Closed	--	101	--	31	--	72	--	293	58.9±17.3
Producer's Accuracy		57.9±41.8	83.8±12.4	69.5±45.2	90±7.3	55.6±44.5	89±6.5	49.2±25.7	63.8±17.2	

Table 7. Confusion matrix for the agriculture layer based on cross-validation. User and producer accuracies with their standard errors are also shown for each class.

PRED \ TRUE	Natural	Agriculture	User's Accuracy
Natural	1109	531	67.6±19.5
Agriculture	25	821	97±3.3
Producer's Accuracy	97.7±2.6	60.7±14.8	

Table 8. Confusion matrix for the wetland layer for both the woody wetland and herbaceous wetland classifications based on cross-validation. User and producer accuracies with their standard errors are also shown for each class. Note that confusion is only possible within the woody or herbaceous wetland sub-groupings.

PRED \ TRUE		Dryland		Wetland		User's Accuracy
		Herb	Woody	Herb	Woody	
Dryland	Herb	1584	--	178	--	89.9±7.3
	Woody	--	2845	--	121	95.6±2.8
Wetland	Herb	41	--	683	--	94.3±7.9
	Woody	--	289	--	211	42.2±20
Producer's Accuracy		97.4±2.7	90.1±3.4	79.3±19.4	63.6±17.3	

Table 9. Comparison between the user and producer accuracies and standard errors for specific classes according to the hierarchical approach (HIER) and an all-in-one classification (ALL). The tree open - deciduous broadleaf class was omitted by the ALL classification. Note the results for the hierarchical approach are not identical to the confusion matrices presented in Tables 4-8, which had been adjusted for the two sources of bias described in Section 2.3.

		User's Accuracies (Errors of Omission)		Producer's Accuracies (Errors of Commission)	
		HIER	ALL	HIER	ALL
Barren		86±13	68±23	89±11	92±7
Snow/Ice		100±0	66±53	4±3	4±3
Water		96±7	99	99	99±1
Tree Closed	Evergreen Needleleaf	87±11	65±17	85±12	81±14
	Deciduous Needleleaf	93±8	75±16	93±7	83±11
	Deciduous Broadleaf	88±10	86±10	89±7	89±8
	Mixed	62±18	59±16	62±17	63±16
Tree Open	Evergreen Needleleaf	79±26	32±27	63±31	17±11
	Deciduous Needleleaf	82±22	56±29	66±38	40±30
	Deciduous Broadleaf	36±50	--	53±47	--
	Mixed	25±24	36±35	42±28	22±24
Shrub Closed		77±20	71±22	32±18	33±19
Shrub Open		36±33	53±28	37±20	51±23
Herbaceous Closed		82±12	83±12	89±6	95±3
Herbaceous Open		73±22	69±24	38±33	32±30

Figures

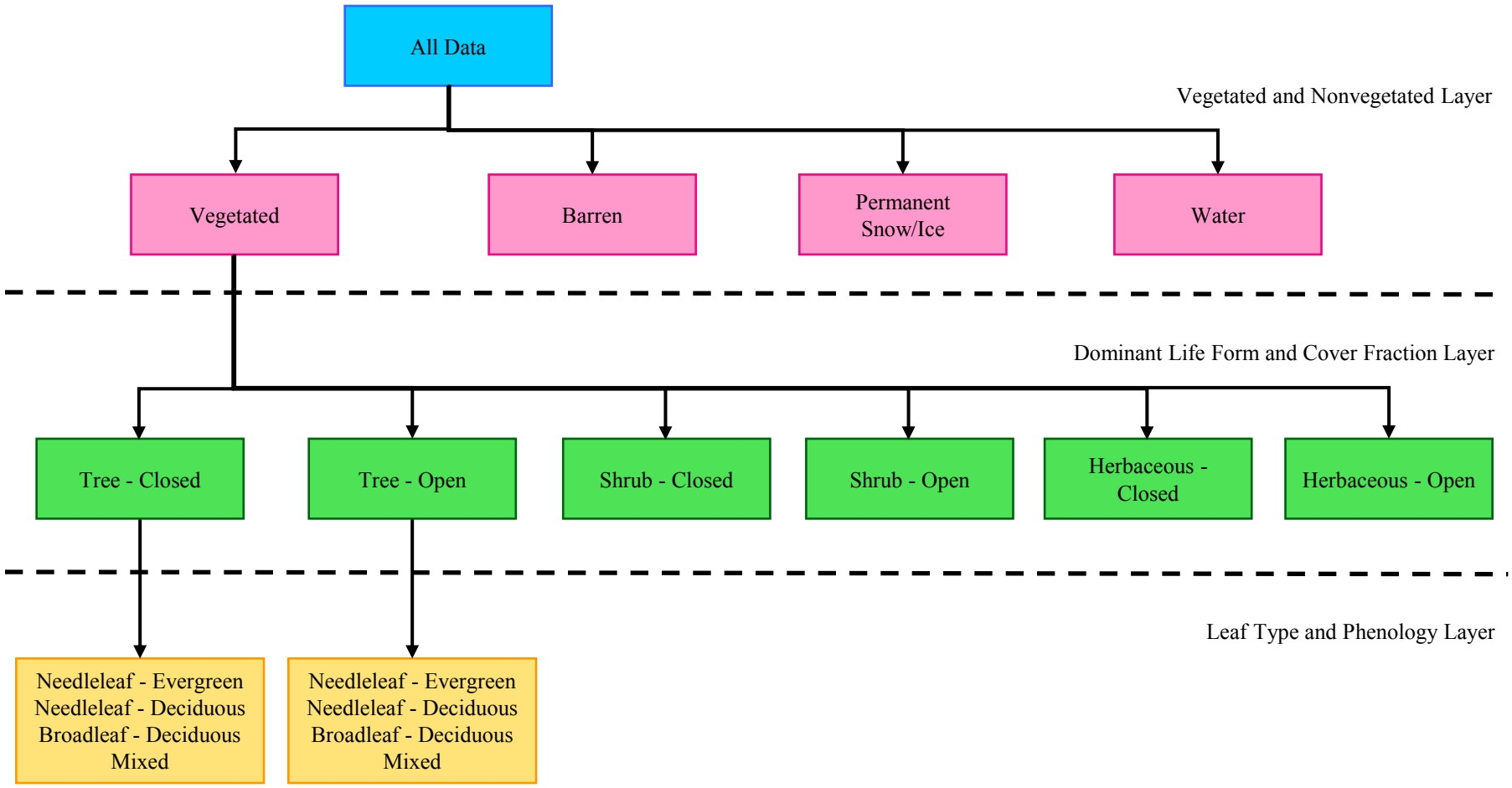

Figure 1. Hierarchical structure of the NELC land cover legend. Dashed lines separate different levels in the hierarchy. The land-use, wetland, and tundra layers (not shown) are complementary to the land cover hierarchy.

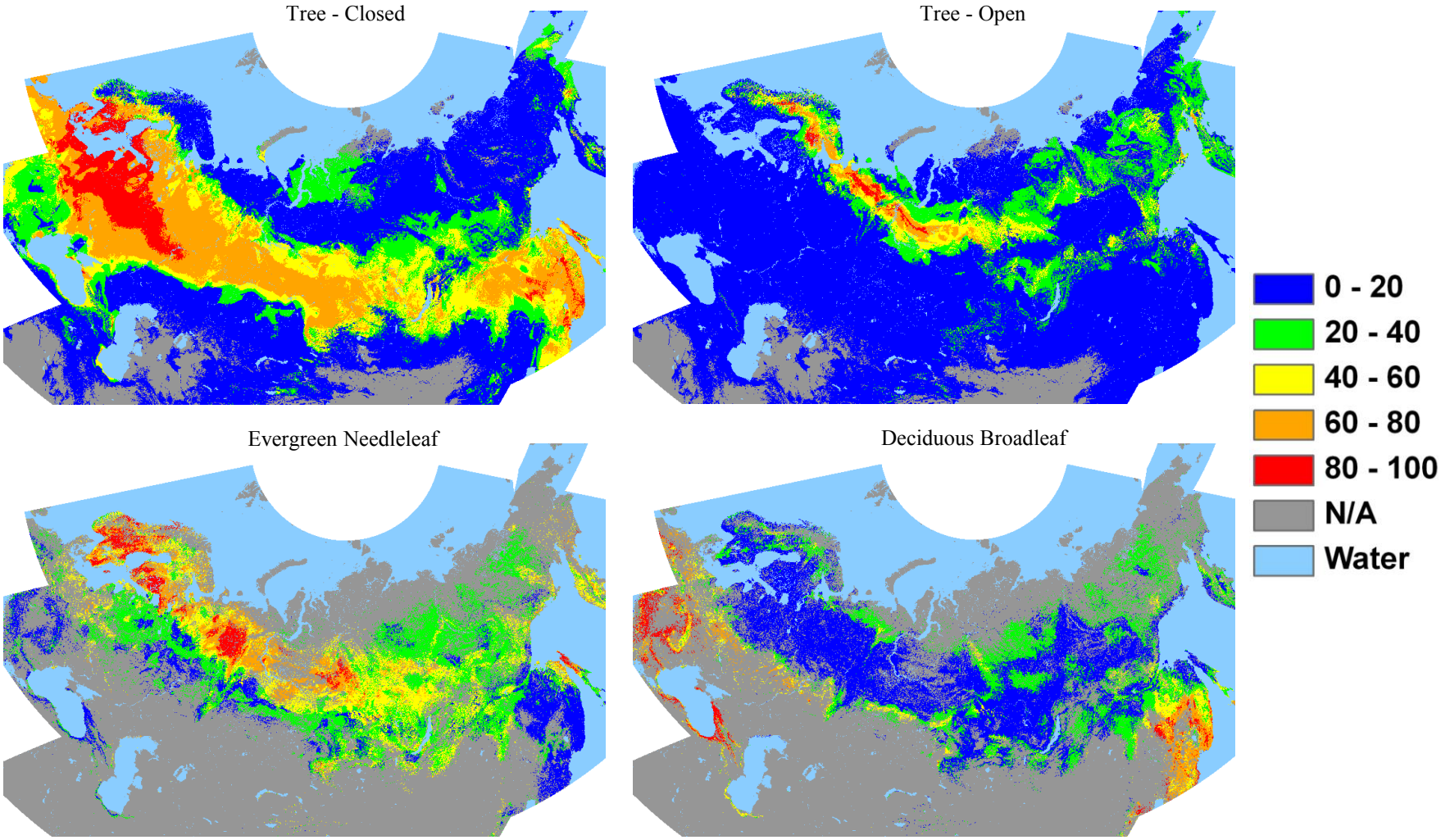

Figure 2. Prior probability layers derived from climate-vegetation relationships for selected classes. The range of values for each color refers to 100 x the probability (%) of a class' presence at a specific pixel location.

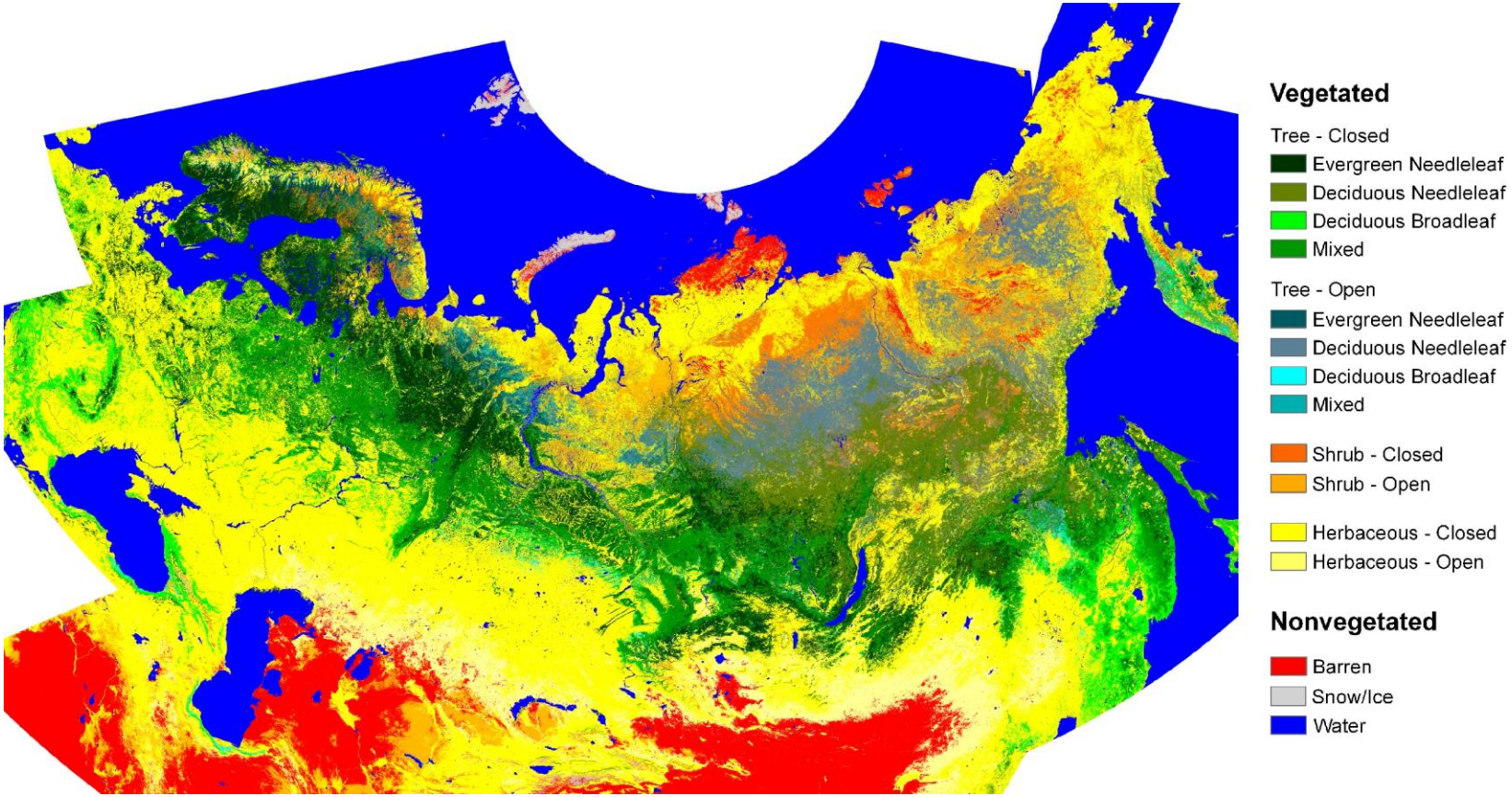

Figure 3. Thematic representation of the 15 land cover classes of the NELC legend. Land use, wetlands, and tundra classes are not shown.

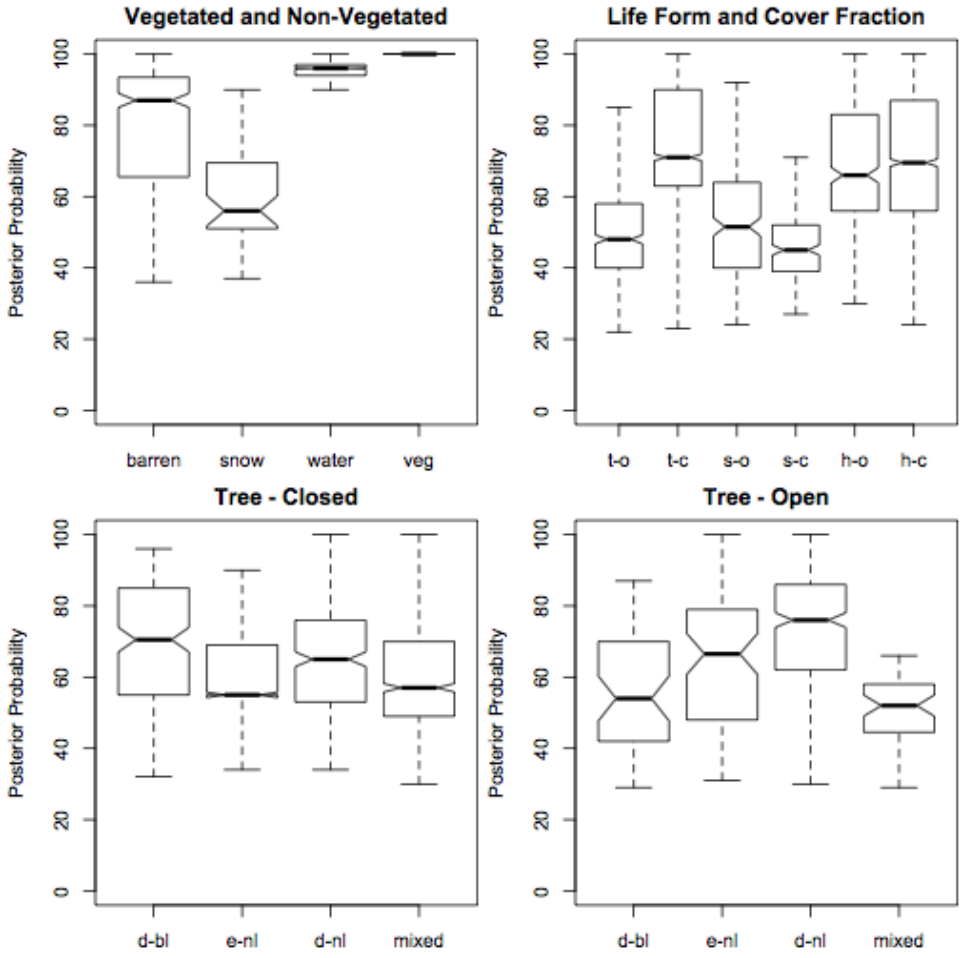

Figure 4. Boxplots showing the distribution of posterior probabilities for each land cover class across a random sample of pixels. For the vegetated and non-vegetated layer: veg refers to vegetated land. For the dominant life form and cover fraction layer: t-o refers to tree-open, t-c to tree-closed, s-o to shrub-open, s-c to shrub-closed, h-o to herbaceous-open, and h-c to herbaceous-closed. For the leaf type and phenology layers: d-bl refers to deciduous broadleaf, e-nl to evergreen needleleaf, and d-nl to deciduous needleleaf.

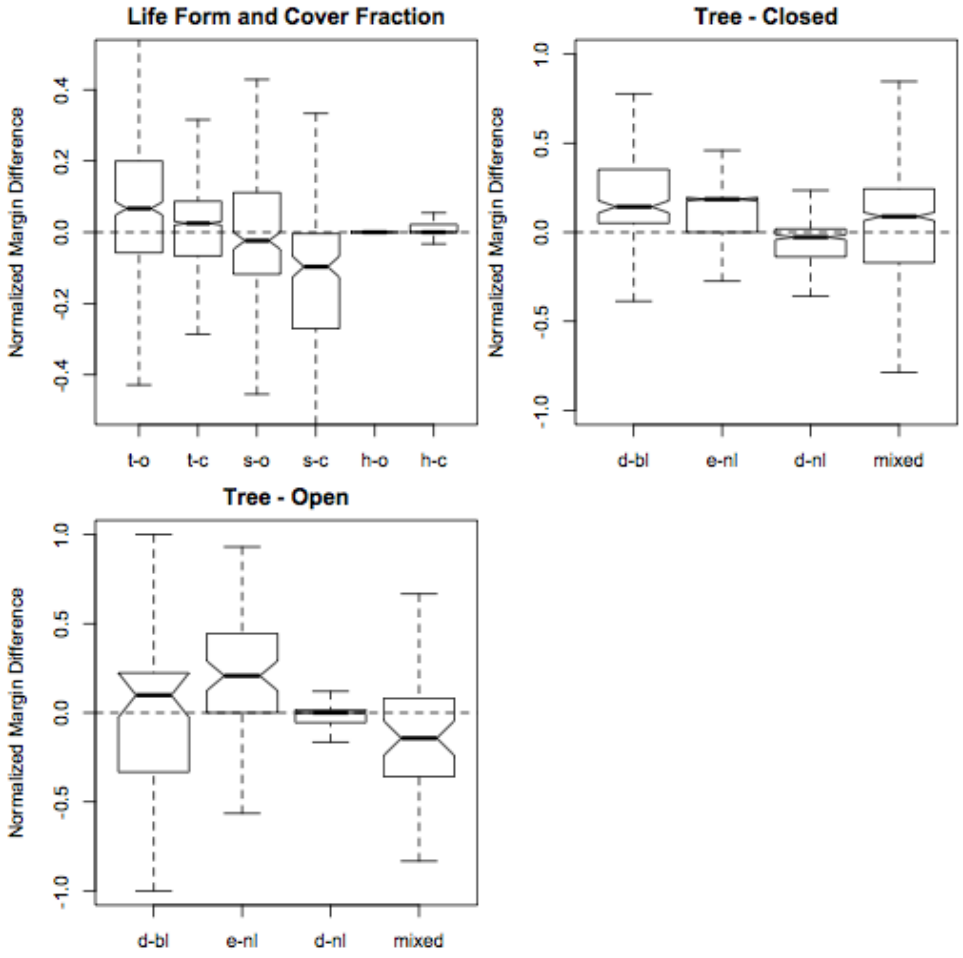

Figure 5. Boxplots showing the distribution of the Normalized Margin Difference (NMD) metric across a random sample of pixels. The NMD quantifies the relative influence of the climate-derived prior probability layers on the final posterior probabilities. For the dominant life form and cover fraction layer: t-o refers to tree-open, t-c to tree-closed, s-o to shrub-open, s-c to shrub-closed, h-o to herbaceous-open, and h-c to herbaceous-closed. For the leaf type and phenology layers: d-bl refers to deciduous broadleaf, e-nl to evergreen needleleaf, and d-nl to deciduous needleleaf.